PREPARATION AND CHARACTERIZATION OF FERRITE NANOPARTICLES FOR THE TREATMENT OF INDUSTRIAL WASTE WATER

V. MANIMOZHI[a*], N. PARTHA[a], E. K. T. SIVAKUMAR[b], N. JEEVA[c],
V. JAISANKAR[c]
[a]Department of Chemical Engineering, Anna University, Chennai – 600025,
Tamil Nadu, India
[b]Centre for Nanoscience and Technology,   Anna University, Chennai – 600025,
Tamil Nadu, India
[c]PG and Research Department of Chemistry,Presidency College (Autonomous),
Chennai-600 005, India

The presence of heavy metals ions in the industrial waste water has a real threat to the environment and public health, because of their toxicity. Nanomaterials became potential for the removal of these toxic metals from waste water. In this paper, we report the synthesis of barium and nickel ferrite nanoparticles by co-precipitation method. The prepared nanoparticles were characterized by Fourier transform infrared (FTIR) spectroscopy, thermogravimetric analysis (TGA), X-ray diffraction (XRD) analysis and scanning electron microscopy (SEM). The preparedferrite nanoparticles have been utilized as adsorbent for Cu^{2+}, Cd^{2+} and Pb^{2+}. The effect of contact time, adsorbent dosage and pH were examined. The experimental results suggest that the proposed ferrite nanoparticles have great potentialfor removal of toxic heavy metal ions from industrial waste water. The kinetic study shows that adsorption process is controlled by pseudo fiirst second order rate equation.

1. Introduction

Water pollution is of great concern since water is the inevitable requisite for the survival of all living organisms. Water pollution has become a continuous increasing problem on the earth which is putting lives in danger. Among the various water pollutants, heavy metal ions require special attention because of their toxic effect on humans and the environment. Unlike organic pollutants, the majority of which are susceptible to biological degradation, heavy metal ions do not degrade into harmless end products [1]. The increased use of heavy metals industrially resulted in an increase in the availability of metallic substances in natural water source [2]. The sources of metal ion pollutants are wastewaters of mining industries, paints and pigment industries, fertilizer industries, metal plating industries, batteries and tannery industries [3]. A large number of elements fall into this category, but lead, copper and cadmium ions are those of relevance in the environmental context. The minimum concentration limit (MCL)standards, for Cu, Cd and Pb established by United States Environmental Protection Agency (USEPA) are 0.25, 0.01 and 0.006 mg/L respectively [4, 5]. Removal of these heavy metal ions from industrial waste water has become necessary as its toxicity in human leads to disruption of the biosynthesis of hemoglobin, rise in blood pressure, kidney damage, miscarriages and abortions, brain damage and learning disabilities in children[6]. Commonly used methods for the removal of heavy metals from aqueous solutions are chemical precipitation, flocculation, reverse osmosis, ion exchange, electro deposition and filtration [7]. Most of these methods have several disadvantages such as chemical requirements, time consuming procedure, production of large amount of sludge, low efficiency and

---

* Corresponding author: mmozhi@gmail.com

less cost effective [8]. However, adsorption method is considered to be more efficient, cost effective and free from sludge formation.

Nanomaterials have a wide range of applications, as in the technological and environmental challenges in the areas of solar energy conversion, catalysis, medicine, and water treatments [9]. Several studies have addressed that nanoparticle specially metal oxide nanoparticles are effective and efficient adsorbents in the cleanup of environmental contaminants, mainly because nanoparticles can penetrate into the contamination zone where microparticles cannot [10]. In this regard, ferrites nanoparticles has opened a new and exciting research field, with revolutionary applications not only in the electronic technology but also in the field of environmental remediation.

The present investigation deals with the synthesis and characterisation of barium and nickel ferrite nanoparticles by co-precipitation method. The synthesized ferrite nanoparticles were characterized using FT-IR, XRD, SEM and TGA. Further, the synthesized barium and nickel ferrite nanoparticles were used as adsorbent to remove heavy metal ions such as copper, cadmium and lead from simulated industrial wastewater. The removal efficiency and adsorption capacity of the synthesized ferrite nanoparticles in removing copper, cadmium and lead were compared. The influence of the factors such as contact time, adsorbent dosage and pH has also been investigated.

2. Experimental methods

2.1 Materials

Ferric chloride, nickel chloride, barium chloride and sodium hydroxide purchased from Merck, were of purity 98-99%. All the chemicals used were analytical grade and used as such.

2.2 Preparation of ferrite nanoparticles

The barium ferrite and nickel ferrite nanoparticles were prepared by simple and inexpensive co-precipitation method [11]. To prepare barium ferrite ($BaFe_2O_4$), aqueous solution of barium chloride and iron chloride hexahydrate(1:2 ratio) were taken in round-bottom flask. To the above solution, 1.5 M aqueous NaOH solution was adding drop by drop with constant stirring. The solution was then refluxed at 80°C for 2 hours. Precipitate was formed which was collected by centrifugation, and washed by distilled water for several times. The obtained product was dried overnight in air oven.

The nickel ferrite ($NiFe_2O_4$)nanoparticles were prepared by the above method using nickel chloride instead of barium chloride and iron chloride. The obtained powder ferrite nanoparticles were used for further characterization.

2.3 Characterization techniques

The metal oxygen bond in the synthesised spinel ferrite nanoparticles was confirmed by Perkin Elmer Model -400 Fourier transform infrared spectrometer. Structure and crystallinity of synthesized nanoparticles was analysed by GEOL JDX -8P X-ray diffractometer having CuKα radiation. The morphology and particle size of the samples were determined from Scanning electron microscopy(SEM Model LEICA S430) .The Thermal stability was evaluated using Thermo Gravimetric analysis(DSC/TGA-Model STA 1640).

2.4 Preparation of simulated industrial wastewater

The 1000 ppm standard solution of copper, cadmium and lead were prepared by dissolving appropriate quantities of their respective salts in distilled water. The simulated wastewater was prepared by using measured amount of standard solutions. The concentration of simulated industrial wastewater Cu^{2+}, Cd^{2+} and Pb^{2+} were 20ppm, 10ppm and 5ppm respectively.

2.5 Adsorption experiment

Adsorption experiment was done by measuring 25mL of the wastewater sample and poured into a 100mL conical flask. 0.1 g of the synthesized barium and nickel nanoparticles were added to different conical flask containing 25mL of wastewater. The conical flask containing the

adsorbent and the wastewater was placed on a rotary shaker and shook at 120 rpm at a room temperature for a period of 180min to ensure equilibrium. The suspension was filtered using 0.5 micron filter paper. Atomic adsorption spectro-photometer (AAS) was used to analyse the concentration of the different metal ions present in the filtrate [12-16]. The influence of the factors such as pH, adsorbent dosage and contact time has been investigated. The effect of contact time on removal of metal ions was studied for the period of 180 minutes at 30 minutes interval under the specific condition (Temp = 30 °C, agitation speed = 120rpm and adsorbent dose = 0.1 g, pH = 6). The effect of pH on adsorption of metal ions in the pH range of 2-8 was studied under the specific condition (Temp = 30 °C, agitation speed = 120rpm, adsorbent dose = 0.1 g and contact time = 150 min). Adsorbent dosage was varied from 0.05 to 0.20 g, under the specific condition (contact time of 150 min, 120 rpm shaking speed and room temperature and pH of 6) using both barium ferrite and nickel ferrite nanoparticles. The amount of metal ions adsorbed by the adsorbent was evaluated using equation (1):

$$q_t = \frac{(C_0 - C_t)V}{W}$$
(1)

The mass balance equation was used to determine the adsorption capacity (q_e) from equation (2):

$$q_e = \frac{(C_0 - C_e)V}{W}$$
(2)

Where, C_o and C_t are the initial and final concentrations of the heavy metals present in wastewater before and after adsorption, for a period of time t (mg/L) respectively: C_e represents the concentration of heavy metals in wastewater (mg/L) when equilibrium was attained. The volume of wastewater used is represented by V (lit) while W represents the mass (g) of the adsorbent used. The percentage of metal ions removed was obtained from equation (3):

$$R(\%) = \frac{(C_0 - C_t) \times 100}{C_0}$$
(3)

where (R %) is the ratio of difference in metal concentration before and after adsorption.

2.6 Effect of contact time on adsorption
The effect of contact time on removal of metal ions was studied for the interval of 30 minutes up to 180 minutes. 0.1 g of the barium and nickel ferrite nanoparticles adsorbents were added to separate conical flask containing 25mL of wastewater. The flask was closed and placed in a rotary shaker, and agitated at speed of 120 rotation per minute (rpm), for each of the different contact times chosen (30, 60, 90,120, 150 and 180 min). The content of each flask was filtered and analyzed using Atomic Absorption Spectroscopy after each agitation time [17].

2.7 Effect of adsorbent dosage on adsorption
Different dosages of the adsorbents (0.05-0.25g) were added in different conical flasks containing 25mL of simulated industrial wastewater solution, corked and agitated in a shaker for 180 min at a speed of 120 rotations per minute (rpm) at a room temperature of 32°C. The content of each flask was then filtered and analyzed using Atomic Absorption Spectroscopy after the agitation time [18].

2.8 Effect of pH on adsorption
The effect of pH on adsorption of metal ions in the pH range of 2-8 was studied. For this investigation, 25 mL of simulated industrial wastewater was taken into different 100 mL conical flask and 0.1 g of the barium and nickel ferrite nanoparticles were added and agitated at a speed of

120 rpm for one hour. The0.5 micron filter paper was used to filter the mixture and the filtrate analyzed to determine the concentrations of metal ions using Atomic Absorption Spectroscopy [19, 20].

3. Results and Discussion

3.1 FT-IR analysis

The FT-IR spectra of the nickel and barium ferrite nanoparticles are shown in Fig. 1.The corresponding stretching vibrations of –OH group is obtained at 3360 cm^{-1}. The peaks at 1598-1618 cm^{-1} indicates flexible vibrations of –OH groups caused by adsorbed water or humidity which shows that the surface of the samples contain active –OH groups. The peaks in the range of 828 to 764 cm^{-1}corresponds to metal-oxygen (Fe-O) stretching vibrations .
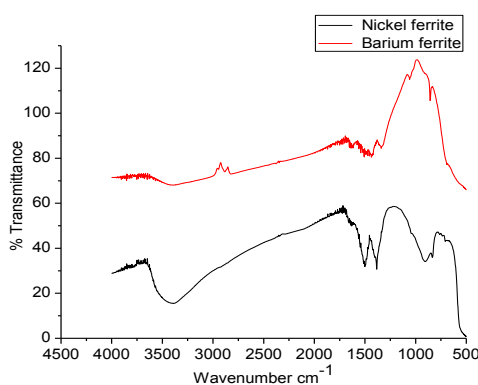
Fig. 1: FTIR spectra of (a) NiFe$_2$O$_4$ and (b) BaFe$_2$O$_4$ nanoparticles.

3.2 XRD analysis

The X-ray diffraction patterns of the synthesized nickel and barium ferrite nanoparticles are shown in Fig. 2(a) and (b) respectively. It shows that the synthesized sample has spinel cubic structure. The significant peak broadening indicates the ultra-fine nature of the sample. The average crystalline diameter (D) was calculated by Scherrer's equation,

$$D = 0.9\lambda/\beta\cos\theta$$

Where, β is the line broadening at the full-width at half maximum (FWHM) of the most intense peak, θ is the Bragg angle and λ is the X-ray wavelength. The average crystalline size of barium and nickel ferrite nanoparticle, were calculated as 72 and 34 nm respectively.
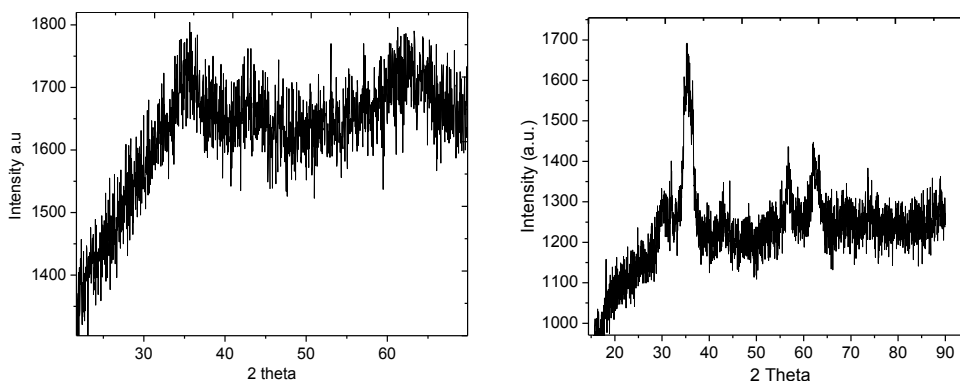
Fig. 2: XRD patterns of (a) NiFe$_2$O$_4$and (b) BaFe$_2$O$_4$nanoparticles.

3.3 SEM analysis

The SEM images of nickel and barium ferrite nanoparticles are shown in Fig. 3(a) and (b) respectively. It results shows that sample exhibit a compact arrangement of homogeneous nanoparticles with spherical in shape. It has been observed that the particles are not aggregated, having almost uniform size distribution and the average size of nickel ferrite is 26 nm and barium ferrite is 73 nm.
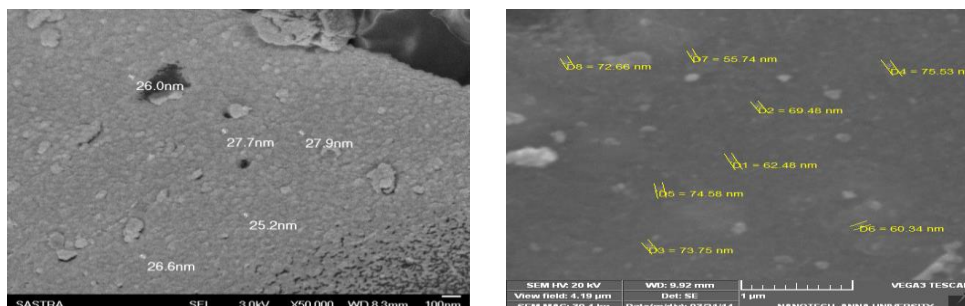
Figure 3: SEM images of (a) $NiFe_2O_4$ and (b) $BaFe_2O_4$ nanoparticles.

3.4 TGA analysis

Thermogram of synthesized nickel and barium ferrite nanoparticles are shown in Fig. 4. The synthesized ferrite nanoparticles were heated from $100^{o}C$ to $900^{o}C$ under N_2 flowing and changes in mass losses are recorded. The weight loss observed at $200^{o}C$ to $300^{o}C$ is due to the evaporation of hydroxyl groups which were adsorbed on the surface of nanoparticles. The broadened exothermic peak at $780^{o}C$ and $800^{o}C$ with small weight loss could be considered as a solid reaction attributed to the gradual formation of nickel and barium ferrite .Above $850^{o}C$, no further distinguishable weight loss was detected.
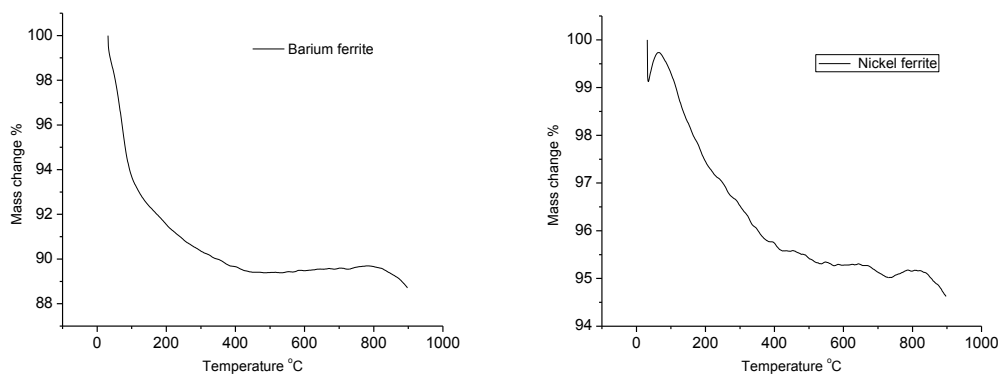
Fig. 4: Thermogram of (a) $NiFe_2O_4$ and (b) $BaFe_2O_4$ nanoparticles.

3.5 Effect of contact time on adsorption of heavy metals

The effect of contact time on the removal efficiency of copper, cadmium and lead ions using synthesized barium and nickel ferrite nanoparticles were studied at room temperature and the obtained results were shown in Fig. 5(A-C).
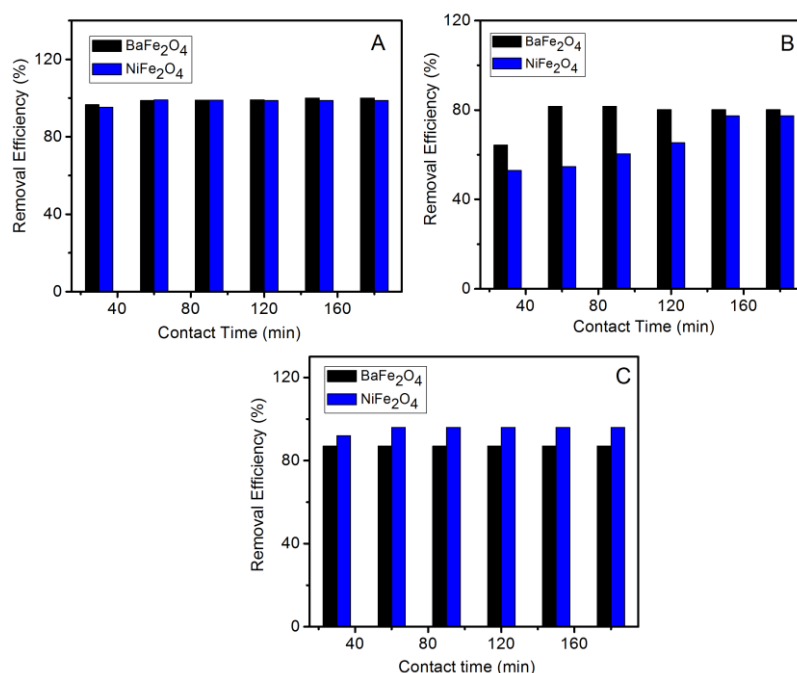
Figure 5:Effect of contact time on adsorption of (A) Cu^{2+}, (B)Pb^{2+}, and (C) Cd^{2+} ions by NiFe$_2$O$_4$ and BaFe$_2$O$_4$ nanoparticles (Temp = 30 °C, agitation speed =120rpm, adsorbent dose = 0.1 g, pH = 6).

From the obtained result, it is evident that the removal of metal ions increases with increase in contact time and attained equilibrium at 180 min, after which further increase in time did not bring about any further improvement for the removal of metal ions, but resulted in desorption of metal ions from the adsorbent surface. Barium ferrite nanoparticles shows maximum removal efficiency of 100% for Cu^{2+} ions in 150 min, 87% for Cd^{2+} ions in 30 min, 81.68% for Pb^{2+} ions in 60 min whereas Nickel ferrite nanoparticles shows maximum removal efficiency of 99.05% for Cu^{2+} ions in 60 min, 96% for Cd^{2+} ions in 60 min,77.47 % for Pb^{2+} ions in 150 min. The results clearly shows that the different metal ions attained equilibrium at different times and the higher removal efficiency is for the removal of Cu^{2+} and lower removal efficiency is for the removal of Pb^{2+}.

3.6 Effect of adsorbent dosage on adsorption of heavy metals

The availability and accessibility of adsorption site is controlled by adsorbent dosage. Adsorbent dosage was varied from 0.05 to 0.20 g, under the specific condition (contact time of 150 min, 120 rpm shaking speed, room temperature and pH of 6) using both Barium ferrite and Nickel ferrite nanoparticles. The relationship between adsorbent dosage and removal efficiency of metal ions from simulated industrial wastewater are shown in the Figure 6.

Barium ferrite nanoparticles shows maximum removal efficiency of 100% for Cu^{2+} ions on 0.1g of adsorbent dosage, 97.7% for Cd^{2+} ions on 0.1g of adsorbent dosage, 80.30% for Pb^{2+} ions on 0.05g whereas Nickel ferrite nanoparticles shows maximum removal efficiency of 99.05% for Cu^{2+} ions on 0.1g of adsorbent dosage, 77.47 % for Cd^{2+} ions on 0.1g of adsorbent dosage, 78 % for Pb^{2+} ions on 0.05g of adsorbent dosage. The results clearly shows that the increase in adsorbent dosage also increases the removal efficiency of metal ions and maximum removal efficiency was attained at a particular adsorbent dosage, after which further increase in adsorbent dosage, brought no increase in adsorption, which was as a result of overlapping of adsorption sites due to overcrowding of adsorbent particles.
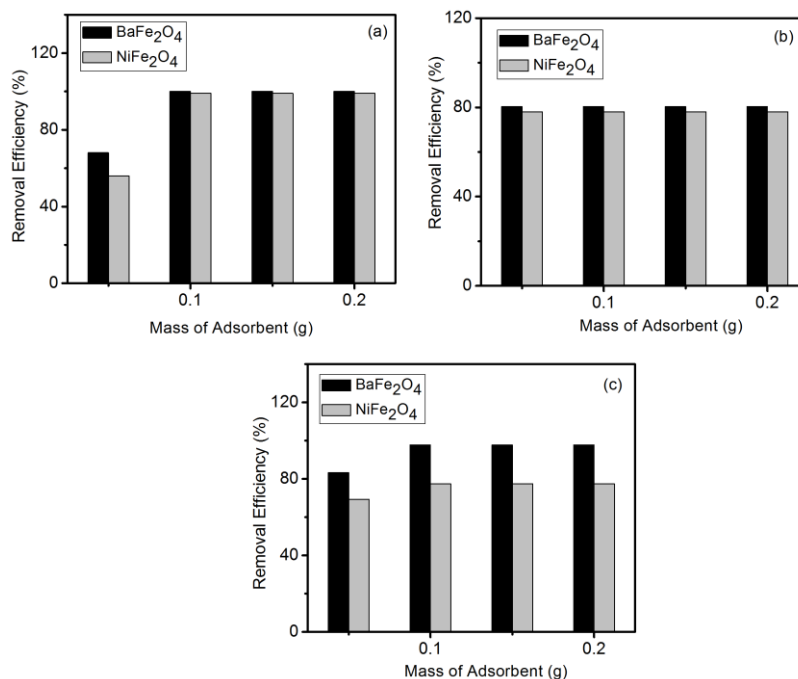
Figure 6: Effect of adsorbent dosage on adsorption of (A) Cu^{2+}, (B) Pb^{2+}, and (C) Cd^{2+} ions by $NiFe_2O_4$ and $BaFe_2O_4$ nanoparticles (Temp = 30 °C, agitation speed =120 rpm, adsorbent dose = 0.1 g, pH = 6).

3.7 Effect of pH on adsorption of heavy metals

The pH of the wastewater is one of the imperative factors governing the adsorption of the metal ions. The effect of pH was studied from a range of 2 to 8 under the precise conditions (at optimum contact time 180 min, 120 rpm shaking speed, with 0.1g of the adsorbent used and at room temperature). Effect of pH on adsorption of metal ions using barium and nickel ferrite nanoparticles was shown in Fig. 7.

It was observed that with increase in the pH from 2 to 6 of the simulated industrial waste water, the removal efficiencies of Cu^{2+} and Cd^{2+} increased up to 6 and maximum removal efficiency was obtained at pH 6 as shown in the Figure 7(a) and 7(b) for both Barium and Nickel ferrite nanoparticles. Above pH 6, there was no change in removal efficiency of Copper and the removal efficiency of Cadmium was gradually decreased. The maximum removal efficiency of Pb^{2+} was obtained at pH 4 and above pH 4, there was no change in removal efficiency for Barium ferrite nanoparticles. But, slight decrease in removal efficiency was observed for Nickel ferrite nanoparticle. Barium ferrite nanoparticles shows maximum removal efficiency of 100% for Cu^{2+} ions at pH 6, 98.05% for Cd^{2+} ions at pH 6, 77.47% for Pb^{2+} ions pH 4 whereas Nickel ferrite nanoparticles shows maximum removal efficiency of 99.05% for Cu^{2+} ions at pH 6, 95.75 % for Cd^{2+} ions at pH 4, 78 % for Pb^{2+} ions on 0.05 g of adsorbent dosage.
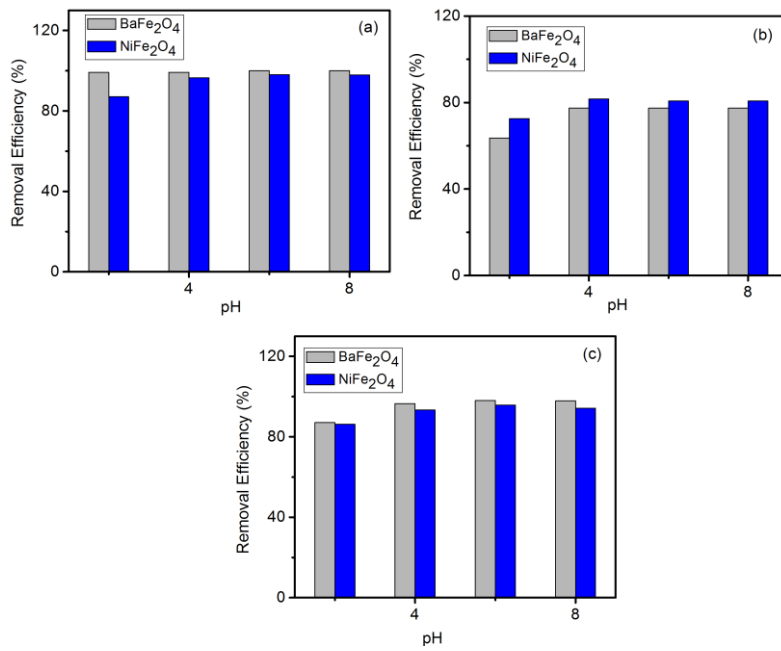
Figure 7: Effect of pH on adsorption of (A) Cu²⁺, (B) Pb²⁺, and (C) Cd²⁺ ions by NiFe₂O₄
and BaFe₂O₄ nanoparticles (Temp= 30 °C, agitation speed=120 rpm, adsorbent dose=
0.1 g, pH = 6).

3.8 Pseudo-first-order kinetic model

The general expression for pseudo-first-order equation model is shown in equation (4) and (5):

$$\frac{dq_t}{dt} = k_1(q_e - q_t) \tag{4}$$

The sorption capacities at equilibrium and at time t, are represented by q_e and q_t respectively (mgg⁻¹) and k_1 is the pseudo-first order sorption rate constant (min⁻¹). Applying boundary conditions after integration, from $t = 0$ to $t = t$ and $q_t = 0$ to $q_t = q_t$, the integrated form of equation becomes

$$\log(q_e - q_t) = \log q_e - \frac{K}{2.303}t \tag{5}$$

The fitted data for Barium and Nickel ferrite nanoparticles of pseudo-first-order reaction model are shown in Fig. 8(a) and 8(b).
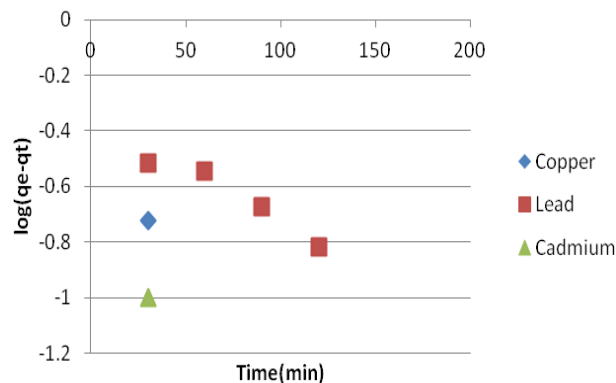
Fig. 8(a) Pseudo-first-order reaction model for adsorption of
heavy metals on Barium ferrite nanoparticles
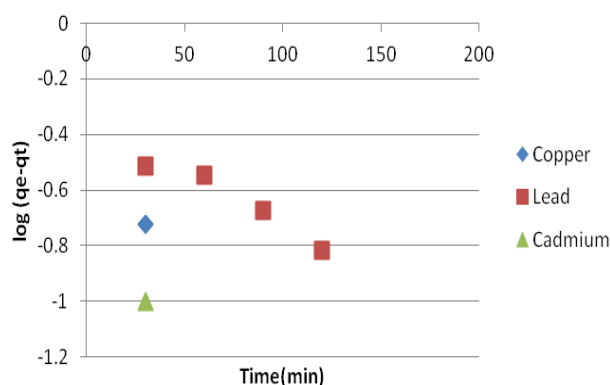
Fig. 8(b) Pseudo-first-order reaction model for adsorption of heavy metals on Nickel ferrite nanoparticles.

From the results of the fitted data, it is clear that the pseudo-first-order reaction model did not yield a straight line, which was significantly scattered. The fact suggests that the adsorption of heavy metal ions by both Barium and Nickel ferrite nanoparticles not follows the pseudo-first - order reaction model.

3.9 Pseudo-second order kinetic model

The pseudo-second order kinetic rate equation is expressed as shown in equation (6)

$$\frac{t}{q_t} = \frac{1}{K_2 q_e^{\ 2}} + \frac{t}{q_e} \tag{6}$$

The sorption capacities at equilibrium and at time t, are represented by q_e and q_t(mgg^{-1}) respectively and k_2 is the rate constant of the pseudo-second order sorption (g.mg^{-1}.min^{-1}). The rate constant and adsorption capacity at equilibrium can be determined experimentally from slope and intercept of the plot.

The fitted data for Barium and Nickel ferrite nanoparticles of pseudo-second-order reaction model are shown in Figure 9(a) and 9(b).
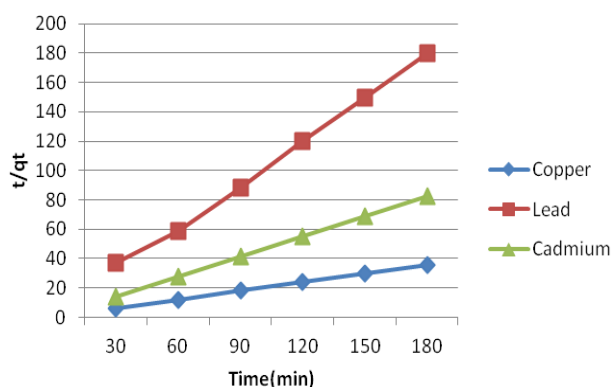
Fig. 9(a) Pseudo-second-order reaction model for adsorption of heavy metals on Barium ferrite nanoparticles
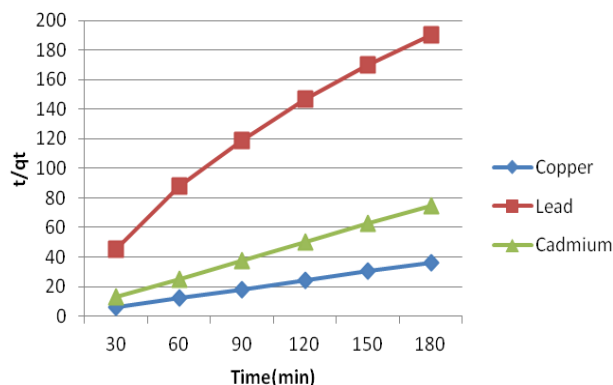
Figure 9(b)Pseudo-second-order reaction model for adsorption of heavy metals on Nickel ferrite nanoparticles

From the results of the fitted data, it is clear that pseudo-second-order reaction model yield very good straight line compared to the pseudo-first-order reaction model, which was significantly scattered (nonlinear). These facts suggest that the adsorption of heavy metals by both Barium and Nickel ferrite nanoparticles follows the pseudo-second-order kinetic model. The equilibrium adsorption capacity (q_e) and the second order constants k_2 (g/mg min) can be determined experimentally from the slope and intercept of plot t/q_t versus t shown Figure 9(a) and 9(b). The k_2 and q_e determined from the pseudo-second-order models of Barium and Nickel ferrite nanoparticles are presented in Table 1 along with the corresponding correlation coefficients.

Table 1. Pseudo-second-order kinetic model for adsorption of heavy metals on Barium and Nickel ferrite nanoparticles

Metal ions	Barium ferrite nanoparticles				Nickel ferrite nanoparticles			
	$q_{e.cal}$ (mg/g)	$q_{e.exp}$ (mg/g)	K_2 (g/mg min)	R^2	$q_{e.cal}$ (mg/g)	$q_{e.exp}$ (mg/g)	K_2 (g/mg min)	R^2
Cu^{2+}	5	5.037	0.1408	0.999	4.95	4.960	0.358	0.999
Pb^{2+}	1.001	1.033	0.2316	0.998	0.96	1.05	0.0339	0.990
Cd^{2+}	2.175	2.175	0.1608	0.999	2.4	2.41	0.4766	1

From the Table 1, it is observed that there is a close agreement between q_e experimental and q_e calculated values for the pseudo-second-order model for both Barium and Nickel ferrite nanoparticles. For example, the calculated q_e value of Cu^{2+} ions using Barium ferrite nanoparticles was 5 mg g^{-1} which is in close agreement with the experimental q_e value of 5.037 mgg^{-1} and the calculated q_e value of Cu^{2+} ions using Nickel ferrite nanoparticles was 4.95 mg g^{-1} which is in close agreement with the experimental q_e value of 4.9603 mg g^{-1}. Hence, the adsorption of heavy metals by both Barium and Nickel ferrite nanoparticles follows the pseudo-second-order reaction model. The correlation coefficients, R^2 values suggest a strong relationship between the parameters and also explain that the process follows pseudo-second-order kinetics.

4. Conclusion

We synthesized barium and nickel ferrite nanoparticles by co-precipitation method. FTIR and XRD analysis confirm the formation of $BaFe_2O_4$ and $NiFe_2O_4$ nanoparticles. The sphere-like morphology of the sample was observed by SEM analysis. Thermal analysis showed that the synthesized nanoparticles have stable over wide range of temperature. Further, the synthesized ferrite nanoparticles were used as adsorbent to remove Cu^{2+}, Cd^{2+} and Pb^{2+} ions from simulated

industrial waste water. Adsorption experimental results shows that the adsorption of Cu^{2+}, Cd^{2+} and Pb^{2+} ions by ferrite nanoparticles depends on contact time, adsorbent dosage and pH. Contact time, adsorbent dosage and pH were optimized as 150 min, 6 and 0.1 g respectively. Barium ferrite nanoparticles show higher removal efficiency for Cu^{2+}, Cd^{2+} and Pb^{2+} than that of nickel ferrite. Kinetic study revealed that the adsorption process of barium and nickel ferrite nanoparticles was controlled by pseudo-second-order rate equation. These results suggest that the ferrite nanoparticles can be effectively used as adsorbents in the commercial scale to achieve the desired goal of clean environment.

References

[1] V.K.Gupta, M. Gupta and S. Sharma, Water Res **35**, 1125 (2001).

[2] S. Tangjuank, N. Insuk, J. Tontrakoon, V. Udeye, World Academy of Science, Engineering and Technology **28**,110 (2009).

[3] K. Jayaram, M.N.V Prasad, J.Hazard.Mater **169**, 991 (2009).

[4] S. Babel, T. A Kurniawan, J. Hazard. Mater **B97**, 219 (2003).

[5] H. Eccles, Trends Biotechnol **17**, 462 (1999).

[6] M. Iram, C. Guo, Y. Guan, A. Ishfaq and H. Liu, J. Hazard. Mater **181**, 1039 (2010).

[7] V. K Gupta, S. Agarwal and T. A Saleh, J.Hazard.Mater **185**, 17 (2011).

[8] M. Shannon, P.W Bohn, M. Elimelech, J.G Georgiadis, B. J Marinas and A. M Mayes Nature **452**, 301(2008).

[9] Q. Liu, T. Zheng, P. Wang, J. Jiang and N. Li, J. Chemical Engineering 157, 348 (2009).

[10] W. Gao, M. Majumder, L. Alemany, N. Tharangattu, A. Miguel, K. Bhebendra M. Pulickel M J. American Chemical Society Appl.Mater. interfaces **3**, 1821(2011).

[11] N. Kannan and M. Sundaram, Dyes and Pigments **51**, 25 (2001).

[12] Z. Chowdhury, S. M Zain and A. K Rashid, J. of Chem. Sci **8**, (1), 333(2010).

[13] M.J Horsfall, A. A Abia, A. I Spiff, J. of Biores Technol **97**, 283(2006).

[14] S. Gopalakrishnan, T. Kannadasan, S. Velmurugan, S. Muthu and P. VinothKumar, Res. J. Chem. Sci **3**, 49 (2009).

[15] O. A Ekpete, F. Kpee, J. C Amadi, R. B Rotimi, R. B, J. of Nep Chem Soc **26**, 32 (2010).

[16] L.I Onyeji and A. A Aboje, Int. J. of EngSci and Technol **3**(12), 8240 (2011).

[17] A. Norhafizahbinti, A. Nurul, R. Imibinti and C. Wong, Asian Trans on Eng **1**(5), 49 (2011).

[18] K. K Jain, P. Guru and V. Singh, *J. of* ChemTechnol Biotech **29**, 36 (1979).

[19] Y. S Ho and G. Mckay, *J.* of Inst of ChemEng Trans **76**, 332 (1998).

[20] W. Rafeah, N. Zainab and U. Veronica, World Applied Sci J **5**, 84 (2009).